Preparation of Nanoscale Ni–B Amorphous Alloys and Their Application in the Selective Hydrogenation of Cinnamic Acid

Guoyi Bai*, Huixian Dong, Zhen Zhao, Yalong Wang, Qingzhi Chen, and Mande Qiu

Key Laboratory of Chemical Biology of Hebei Province, College of Chemistry and Environmental Science,
Hebei University, Baoding, Hebei, 071002, P. R. China

A series of metal modified nanoscale Ni–B amorphous alloys was prepared by chemical reduction and tested in the selective hydrogenation of cinnamic acid. A Co modified Ni–B amorphous alloy (Ni–Co–B) exhibited excellent catalytic performance in this reaction with both 100.0% conversion of cinnamic acid and 100.0% selectivity for hydrocinnamic acid under the optimized reaction conditions. X-ray diffraction (XRD) results indicated that the addition of Co had not changed the amorphous structure of Ni–B; whereas, its addition was believed not only to favor decreased agglomeration of the active Ni species, as proven by transmission electron microscopy (TEM), but also to contribute to adsorption of hydrogen itself. Thus, Ni–Co–B showed a larger BET surface area, smaller particle size, and greater number of active species resulting in optimum H_2-chemisorption compared to Ni–B and accounting for its excellent catalytic performance in cinnamic acid hydrogenation.

Keywords: Nanoscale Amorphous Alloy, Metal Modified, Ni–Co–B, Cinnamic Acid, Selective Hydrogenation.

RESEARCH ARTICLE

1. INTRODUCTION

Nanoscale materials have attracted considerable interest over recent decades due to their unique electrical, optical and catalytic properties.[1] In particular, nanoscale amorphous alloys have been widely used in the field of catalysis and hydrogen storage materials, because of their combination of the attributes of nano materials and amorphous alloys, i.e., short-range order, long-range disorder, and high dispersion.[2–4] Recently, nanoscale Ni–B amorphous alloys have been applied in a series of catalytic hydrogenations,[5–7] but the undoped Ni–B amorphous alloys usually showed poor activities. Consequently, various methods, such as addition of metals,[8–14] polymers,[15, 16] as well as the application of ultrasound,[17–19] have been investigated to control the particle size in order to improve the activity of the Ni–B amorphous alloy. Among them, addition of metals has attracted the most interest due to its efficiency. For instance, Ni–Fe–B and Ni–Ce–B amorphous alloy catalysts prepared by Li et al.[8, 9] have shown excellent activity in the selective hydrogenation of furfural to furfuryl alcohol. Chen et al.[10] have reported that W, Mo, and Ru doped Ni–B amorphous alloys were effective for the catalytic

hydrogenation of *p*-chloronitrobenzene to *p*-chloroaniline, improving activity and stability of the catalyst. Recently, we have found that the incorporation of La into a Ni–B amorphous alloy can introduce more active centers, higher H_2-chemisorption and smaller particle sizes, accounting for the higher activity of Ni–La–B in the selective hydrogenation of benzophenone.[11]

Hydrocinnamic acid, also known as 3-phenylpropionic acid, has attracted much attention as an important pharmaceutical raw material and intermediate.[20] Catalytic hydrogenation of cinnamic acid is the most effective method to obtain hydrocinnamic acid. Pd-based noble metal catalysts, including Pd/PS (polystyrene),[21] Fe_3O_4@Pd,[22] [Pd(NHC)(PCy$_3$)],[23] Pd/MCM-48,[24] Pd/Mg-La mixed oxide,[25] and SiliaCat Pd^0,[26] have been widely applied in the hydrogenation of cinnamic acid and all exhibited high activities. Unfortunately, the high price of noble metal catalysts has limited their further application in industry.[27] Recently, Rao et al.[28] have reported the synthesis of hydrocinnamic acid from the hydrogenation of cinnamic acid over a $NaBH_4$-Raney Ni catalyst with an 89.0% yield; whereas, the potential environmental pollution, mainly from waste alkali solution in the Raney Ni preparation, has become increasingly problematic in industrial applications. Therefore, there remains a need to find a

---
*Author to whom correspondence should be addressed.

suitable catalyst, having low cost, low environmental pollution, and high activity, for the selective hydrogenation of cinnamic acid to hydrocinnamic acid.

To the best of our knowledge, no work on the hydrogenation of cinnamic acid over amorphous alloy catalysts has been reported; so, we report herein our recent research into the hydrogenation of cinnamic acid over nanoscale amorphous alloys. A series of metal modified nanoscale Ni–B amorphous alloy catalysts was prepared and tested in this reaction. A Co modified Ni–B amorphous alloy (Ni–Co–B) exhibited the highest activity among the catalysts studied. Furthermore, the promoting effect of Co on the catalytic activity of Ni–B was studied.

2. EXPERIMENTAL DETAILS

2.1. Catalyst Preparation

The Ni–B amorphous alloy catalyst was prepared by chemical reduction, as shown in Scheme 1. In a typical run, 1 mol/L aqueous KBH_4 containing 0.2 mol/L NaOH (25 mL) was added dropwise to 10 mL of 0.5 mol/L aqueous $NiCl_2 \cdot 6H_2O$ with vigorous stirring and cooling in an ice bath to furnish a black precipitate. Distilled water was then used to wash the resulting black precipitate repeatedly until the washings were pH 7. The catalyst was further washed with absolute ethanol three times to replace residual water and then stored under absolute ethanol. When $CoCl_2 \cdot 6H_2O$ or $X(NO_3)_2 \cdot nH_2O$ (X = La, Ce, Zr, molar ratio Ni:X = 10:1, n = 5 or 6) was also added to the
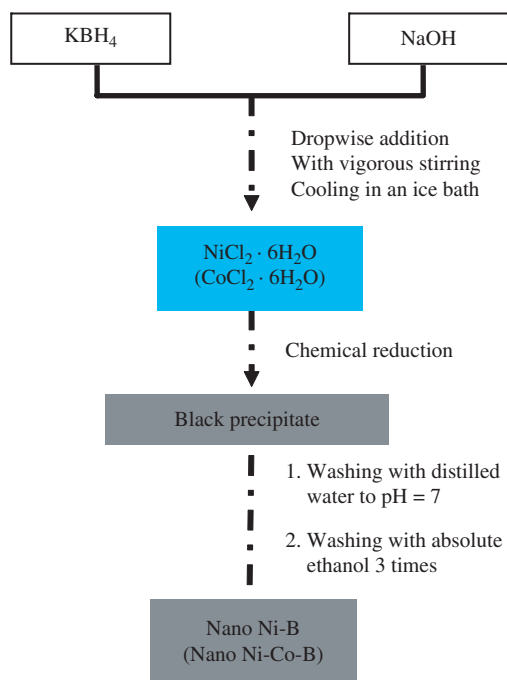
Scheme 1. Flowchart showing the preparation of Ni–B amorphous alloy catalysts.
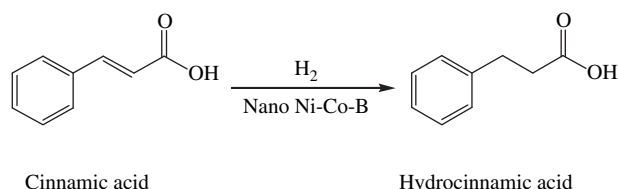
Scheme 2. Hydrogenation of cinnamic acid.

aqueous nickel chloride during the preparation, the catalysts so obtained are denoted as Ni–X–B.

2.2. Catalyst Characterization

Bulk compositions of the amorphous alloy catalysts were measured by inductively coupled plasma analysis (ICP) using a Varian Vista-MPX spectrometer. BET surface area and pore volume were tested on a Micromeritics Tristar II 3020 surface area and pore analyzer. X-ray diffraction patterns (XRD) were recorded with a Bruker D8 diffractometer using Cu Kα radiation. Scanning electron microscopy (SEM) was performed on a JEOL JSM-7500 electron microscope. Transmission electron microscopy (TEM) images were obtained with a FEI Tecnai G2 microscope. H_2-chemisorption and temperature programmed desorption of H_2 (H_2-TPD) were performed on a TP-5000 instrument supplied by Xianquan Ltd.

2.3. Catalyst Activity Test

Cinnamic acid hydrogenation (Scheme 2) was carried out in a 100 mL stainless steel autoclave equipped with a mechanical stirrer and electric heating system. Cinnamic acid (3.0 g), catalyst (0.05 g) and H_2O (60 mL) were briefly mixed in the autoclave and then the reactor was filled with H_2 three times followed by evacuation to exclude residual air. The autoclave was then pressurized with H_2 to 2 MPa, and heated to 100 °C. On reaching 100 °C, hydrogenation was started by stirring the reaction mixture vigorously and allowed to proceed for 1 h. Reaction mixtures were analyzed by gas chromatography using a 30 m SE-30 capillary column and the product structures were confirmed using gas chromatography-mass spectrometry (GC-MS) on an Agilent 5975C spectrometer.

3. RESULTS AND DISCUSSION

3.1. Catalyst Characterization

The bulk compositions, BET surface areas, particle sizes, and H_2-chemisorption of Ni–B and Ni–Co–B amorphous alloy catalysts were measured, and selected results are listed in Table I. From the ICP analysis, it was found that B content increased with the addition of Co, probably due to the additional reduction of Co^{2+} by BH_4^-. The BET surface area and pore volume of the catalyst markedly increased with the addition of Co; whereas, the mean particle size

Table I. Selected physicochemical properties of the Ni–B amorphous alloys.

Catalyst	Composition (atomic ratio)[a]	Surface area (m²/g)	Pore volume (cm³/g)	Particle size (nm)[b]	H₂-chemisorption (cm³/g)
Ni–B	$Ni_{1.00}B_{0.38}$	21.3	0.046	10.7	0.14
Ni–Co–B	$Ni_{1.00}Co_{0.08}B_{0.52}$	28.3	0.062	7.3	0.22

Notes: [a]Based on ICP results; [b]Based on TEM results.
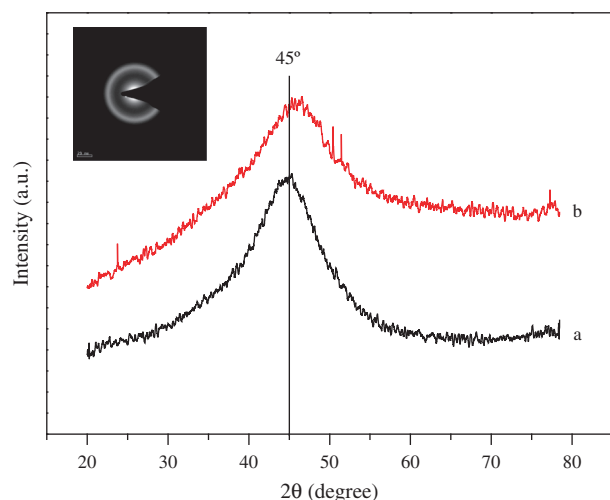

Fig. 1. XRD patterns of the amorphous alloy catalysts. (a) Ni–B, (b) Ni–Co–B. The inset is the SAED image of the Ni–Co–B.

decreased from 10.7 to 7.3 nm at the same time. The H₂-chemisorption value of Ni–Co–B is higher than that of Ni–B, demonstrating that Ni–Co–B possesses more active species.

XRD patterns of Ni–B and Ni–Co–B are shown in Figure 1. A broad peak at around $2\theta = 45°$ was observed for both catalysts indicative of a typical amorphous structure,[29] which can also be confirmed by a successive diffraction halo in an attached SAED image (Fig. 1 inset).[30] It indicated that the addition of Co had not changed the amorphous structure of Ni–B.

Figure 2 shows SEM images of Ni–B and Ni–Co–B. This reveals that the two amorphous alloy catalysts both presented an approximately spherical morphology,

consistent with other reported Ni-based amorphous alloy catalysts.[31] Some agglomeration was observed on the surface of Ni–B, but this phenomenon was inhibited by the addition of Co, accounting for the smaller particle sizes and larger surface area in this preparation.

The morphologies and size distribution of the amorphous catalysts were recorded by TEM (Fig. 3). As can be seen, the particles in the two catalysts are both approximately spherical, in accordance with the SEM results above. There was apparent agglomeration in Ni–B; whereas, this phenomenon was effectively inhibited in Ni–Co–B. Furthermore, the particle distribution also decreased from 6.7–17.9 to 5.0–9.6 nm on the addition of Co. Thus, Ni–Co–B was proven to possess smaller, more uniform, and better dispersed active particles compared to Ni–B.

Figure 4 exhibits the H₂-TPD profiles of the two samples. Ni–B shows two obvious peaks at about 250 and 360 °C, respectively, indicating the presence of two different adsorbing sites. In contrast, Ni–Co–B presents only one strong peak at around 330 °C. Thus, it can be concluded that the active Ni species of the catalyst has a trend to become uniform on the addition of Co, as also reported by Xie et al.[32] Furthermore, it is apparent that the hydrogen desorption peak of Ni–Co–B is much larger than that of Ni–B, in agreement with the H₂-chemisorption results, indicating that the added Co might not only favor the dispersion of the active Ni species but also contribute to adsorption of hydrogen itself.

3.2. Catalyst Selection and Optimization

A series of metal modified amorphous alloy catalysts was prepared and investigated in the hydrogenation of cinnamic acid, and the results are listed in Table II. Surprisingly,
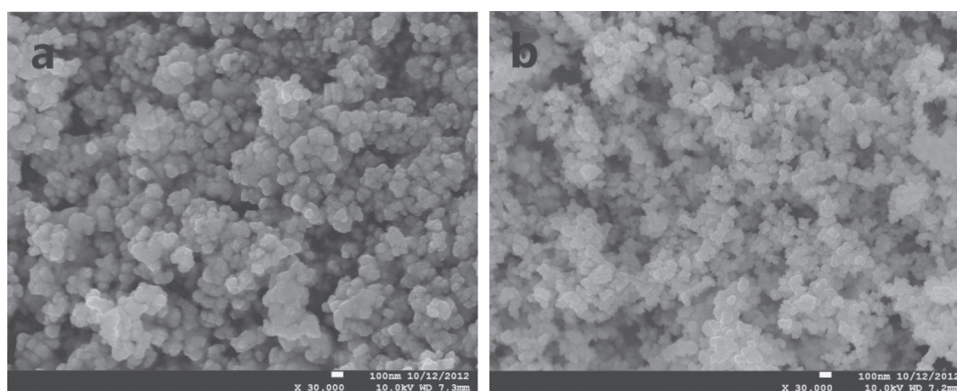

Fig. 2. SEM images of the amorphous alloy catalysts. (a) Ni–B, (b) Ni–Co–B.
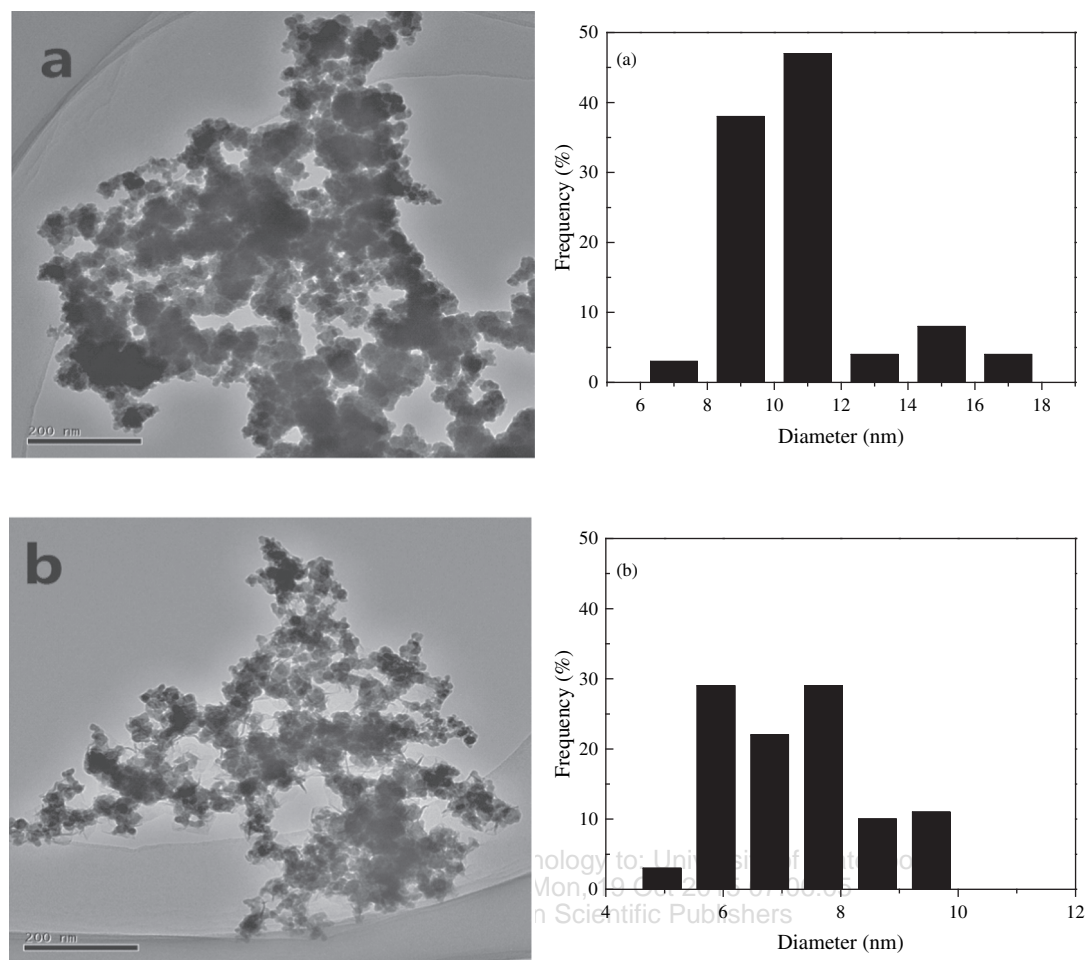
Fig. 3. TEM images and particle size distributions of the amorphous alloy catalysts. (a) Ni–B, (b) Ni–Co–B.

all the amorphous alloy catalysts showed 100.0% selectivity for hydrocinnamic acid. Furthermore, the conversion of cinnamic acid increased from 50.7% to 69.3% with the addition of Co; whereas it unexpectedly decreased with other metal modified amorphous alloys compared to Ni–B. We speculated that the coverage effect of these metal additives should play a more significant role than their dispersion effect on the active Ni centers of the Ni–B amorphous alloy in this reaction. In contrast, in the case of Ni–Co–B, the added Co was believed not only to disperse the active Ni species of the Ni–B amorphous alloy, but also to take part in the hydrogenation process itself. Thus, the Co–B amorphous alloy was also tested in cinnamic acid hydrogenation for comparison and gave 46.2% cinnamic acid conversion, similar to that of the undoped Ni–B, but markedly lowered than that of Ni–Co–B. Thus, there must be certain positive synergistic effects between Ni and Co, as indicated by the H_2-chemisorption and H_2-TPD results, accounting for the higher activity of Ni–Co–B, as also reported by Lekgoathi et al. in the hydrogenation of unsaturated fatty acid methyl esters obtained from avocado oil.[33] Consequently, Ni–Co–B was chosen as the best catalyst for cinnamic acid hydrogenation.

Initially, the effect of hydrogen pressure was investigated to achieve a better conversion of cinnamic acid over the Ni–Co–B catalyst. It was apparent that the conversion of cinnamic acid increased remarkably with the
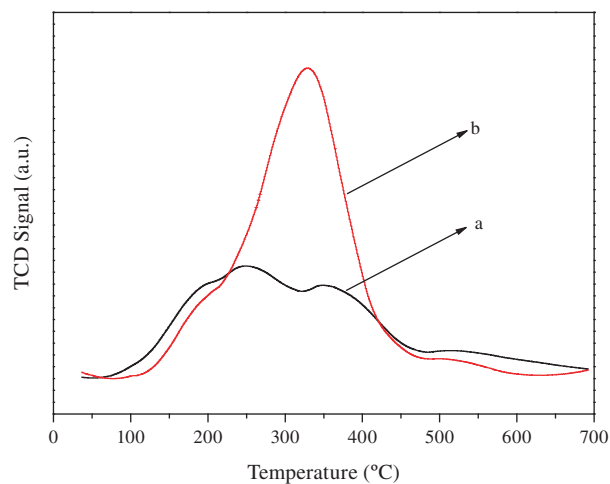

Fig. 4. H_2-TPD spectra of the amorphous alloy catalysts. (a) Ni–B, (b) Ni–Co–B.

RESEARCH ARTICLE

Table II. Hydrogenation of cinnamic acid over the Ni–B and Ni–Co–B catalysts.[a]

Catalyst	Conversion of cinnamic acid (%)	Selectivity for hydrocinnamic acid (%)
Ni–B	50.7	100.0
Ni–La–B	32.2	100.0
Ni–Ce–B	29.9	100.0
Ni–Zr–B	50.0	100.0
Ni–Co–B	69.3	100.0
Co–B	46.2	100.0

Notes: [a]Reaction conditions: 3.0 g cinnamic acid, 0.05 g catalyst, 60 mL H_2O, temperature at 100 °C, initial $P(H_2) = 2$ MPa, and reaction time 1 h.

increase of hydrogen pressure. A 91.0% conversion could be achieved with a hydrogen pressure of 3 MPa and complete conversion could be achieved at a hydrogen pressure of 5 MPa. Considering safety issues and the feasibility of further applications, 3 MPa was selected as the appropriate reaction pressure. Subsequently, the effect of reaction temperature on the conversion of cinnamic acid was examined. The conversion of cinnamic acid increased from 91.0% to 100.0%, when the reaction temperature was increased from 100 to 120 °C and so 120 °C was chosen as the optimum reaction temperature. Thus, the conversion of cinnamic acid and the selectivity for hydrocinnamic acid were both 100.0% over Ni–Co–B under the optimized reaction conditions, superior to that of Ni–B (85.9%) under the same conditions, and the same as the results of Pd-based catalysts.[21, 24]

4. CONCLUSIONS

In conclusion, a series of metal modified nanoscale Ni–B amorphous alloy catalysts was prepared by chemical reduction and investigated in the selective hydrogenation of cinnamic acid. Ni–Co–B showed the best catalytic performance with both 100.0% conversion and selectivity for hydrocinnamic acid. The addition of Co was believed not only to favor decreased agglomeration of the active Ni species but also to contribute to adsorption of hydrogen itself, resulting in the Ni–Co–B having smaller particle size, larger BET area, higher H_2-chemisorption, and greater number of active species, accounting for its excellent catalytic performance. Due to its good activity, environmentally friendly nature and low cost, the catalytic system involving of Ni–Co–B is a potential catalyst of choice to produce hydrocinnamic acid in large-scale processes.

References and Notes

1. L. J. Lauhon, M. S. Gudlksen, D. L. Wang, and C. M. Lieber, *Nature* 420, 57 (**2002**).
2. J. F. Deng, H. X. Li, and W. J. Wang, *Catal. Today* 51, 113 (**1999**).
3. B. J. Liaw, S. J. Chiang, S. W. Chen, and Y. Z. Chen, *Appl. Catal. A: Gen.* 346, 179 (**2008**).
4. A. S. Kumar, K. K. R. Datta, T. S. Rao, K. V. Raghavan, M. Eswaramoorthy, and B. V. S. Reddy, *J. Nanosci. Nanotechnol.* 12, 2000 (**2012**).
5. Y. Z. Chen, B. J. Liaw, and S. J. Chiang, *Appl. Catal. A: Gen.* 284, 97 (**2005**).
6. H. Li, H. X. Li, W. L. Dai, W. J. Wang, Z. G. Fang, and J. F. Deng, *Appl. Surf. Sci.* 152, 25 (**1999**).
7. J. B. Zheng, Z. Q. Xia, J. J. Li, W. K. Lai, X. D. Yi, B. H. Chen, W. P. Fang, and H. L. Wan, *Catal. Commun.* 21, 18 (**2012**).
8. H. X. Li, H. S. Luo, L. Zhuang, W. L. Dai, and M. H. Qiao, *J. Mol. Catal. A: Chem.* 203, 267 (**2003**).
9. H. X. Li, S. Y. Zhang, and H. S. Luo, *Mater. Lett.* 58, 2741 (**2004**).
10. L. F. Chen and Y. W. Chen, *Ind. Eng. Chem. Res.* 45, 8866 (**2006**).
11. G. Y. Bai, L. B. Niu, M. D. Qiu, F. He, X. X. Fan, H. Y. Dou, and X. F. Zhang, *Catal. Commun.* 12, 212 (**2010**).
12. J. H. Shen and Y. W. Chen, *J. Mol. Catal. A: Chem.* 273, 265 (**2007**).
13. Y. W. Chen and N. Sasirekha, *Ind. Eng. Chem. Res.* 48, 6248 (**2009**).
14. W. Y. Wang, Y. Q. Yang, H. Luo, H. Z. Peng, and F. Wang, *Ind. Eng. Chem. Res.* 50, 10936 (**2011**).
15. G. Y. Bai, Z. Zhao, L. B. Niu, H. X. Dong, M. D. Qiu, F. Li, Q. Z. Chen, and G. F. Chen, *Catal. Commun.* 23, 34 (**2012**).
16. B. J. Liaw, C. H. Chen, and Y. Z. Chen, *Chem. Eng. J.* 157, 140 (**2010**).
17. K. S. Suslick, S. B. Choe, A. A. Cichowlas, and M. W. Grinstaff, *Nature* 353, 414 (**1991**).
18. J. Guo, Y. J. Hou, C. H. Yang, Y. Q. Wang, H. Q. He, and W. Li, *Catal. Commun.* 16, 86 (**2011**).
19. J. Guo, Y. J. Hou, C. H. Yang, Y. Q. Wang, and L. N. Wang, *Mater. Lett.* 67, 151 (**2012**).
20. K. J. P. Narayana, P. Prabhakar, M. Vijayalakshmi, Y. Venkateswarlu, and P. S. J. Krishna, *Pol. J. Microbiol.* 56, 191 (**2007**).
21. C. M. Park and M. S. Kwon, *J. Park, Synth.* 22, 3790 (**2006**).
22. A. J. Amali and R. K. Rana, *Green Chem.* 11, 1781 (**2009**).
23. V. Jurcik, S. P. Nolan, and C. S. J. Cazin, *Chem. Eur. J.* 15, 2509 (**2009**).
24. S. Banerjee, V. Balasanthiran, R. T. Koodali, and G. A. Sereda, *Org. Biomol. Chem.* 8, 4316 (**2010**).
25. M. L. Kantam, R. Kishore, J. Yadav, M. Sudhakar, and A. Venugopal, *Adv. Synth. Catal.* 354, 663 (**2012**).
26. V. Pandarus, G. Gingras, F. Beìland, R. Ciriminna, and M. Pagliaro, *Org. Process Res. Dev.* 16, 1230 (**2012**).
27. L. F. Mabena, S. S. Ray, S. D. Mhlanga, and N. J. Coville, *Appl. Nanosci.* 1, 67 (**2011**).
28. G. K. Rao, N. B. Gowda, and R. A. Ramakrishna, *Synth. Commun.* 42, 893 (**2012**).
29. Z. B. Yu, M. H. Qiao, H. X. Li, and J. F. Deng, *Appl. Catal. A: Gen.* 163, 1 (**1997**).
30. H. Li, J. Liu, S. H. Xie, M. H. Qiao, W. L. Dai, and H. X. Li, *J. Catal.* 259, 104 (**2008**).
31. H. X. Li, H. Li, W. L. Dai, and M. H. Qiao, *Appl. Catal. A: Gen.* 238, 119 (**2003**).
32. G. W. Xie, W. Sun, and W. B. Li, *Catal. Commun.* 10, 333 (**2008**).
33. M. D. S. Lekgoathi, W. G. Augustyn, and J. Heveling, *J. Nanosci. Nanotechnol.* 11, 7001 (**2011**).

RESEARCH ARTICLE